PHYSICAL REVIEW B **68**, 081303(R) (2003)

Magnetic field in-plane quantization and tuning of population inversion in a THz superlattice quantum cascade laser

Jesse Alton,[1,2] Stefano Barbieri,[2,*] John Fowler,[1,2] Harvey E. Beere,[1] John Muscat,[1] Edmund H. Linfield,[1] David A. Ritchie,[1] Giles Davies,[3] Rüdeger Köhler,[4] and Alessandro Tredicucci[4]

[1]*Cavendish Laboratory, University of Cambridge, Madingley Road, Cambridge CB3 0HE, United Kingdom*

[2]*TeraView Ltd, 302/304 Science Park, Cambridge CB4 0WG, United Kingdom*

[3]*School of Electronic and Electrical Engineering, University of Leeds, Leeds LS2 9JT, United Kingdom*

[4]*NEST-INFM and Scuola Normale Superiore, Piazza dei Cavalieri 7, 56126 Pisa, Italy*

(Received 16 May 2003; revised manuscript received 8 July 2003; published 29 August 2003)

The operation of a 4.4 THz, GaAs-based quantum cascade laser is investigated in a 0–7.5 T magnetic field applied parallel to the growth axis. Pronounced oscillations are found in the threshold current and output power as the magnetic field is increased. At 4.3 T the threshold current density is drastically reduced to 160 A/cm^2 from the 290 A/cm^2 measured at 0 T. We attribute these results to a modulation of the lifetime of the upper state of the laser transition owing to the combined effects of inter-Landau level resonances and a progressive quenching of nonradiative relaxation channels due to the additional in-plane quantization. The latter is also responsible for a dramatic decrease in the conductivity, with a reduction in the number of carriers injected into the upper state of the laser transition at fixed voltage. This process limits the maximum output power and eventually prevents lasing action at high magnetic fields.

DOI: 10.1103/PhysRevB.68.081303 PACS number(s): 76.40.+b, 72.20.My, 42.55.Px

When a magnetic field (B) is applied parallel to the growth axis of a semiconductor heterostructure, each two-dimensional electronic subband is split into a series of zero-dimensional (0-D) Landau levels (LL's). This additional in-plane quantization causes a progressive lowering of non-radiative inter-LL scattering with increasing magnetic field, as a result of the reduced phase-space available.[1–3] This general trend can be reversed when special resonance conditions are obtained either by adjusting the magnetic field or the bias across the structure.[4] One such situation occurs when the inter-LL spacing is equal to the optical phonon energy, yielding enhanced-optical phonon emission. This effect has been recently exploited to modulate the lifetime of the upper state of the laser transition in a quantum cascade laser emitting at 11.2 μm.[5] Increase in the scattering rate can also be obtained when two LL's are brought into resonance, since in this case electrons can scatter elastically as a result of impurity, interface roughness, and carrier-carrier scattering.[4,6,7]

Quantum cascade-type electroluminescent structures based on the GaAs/AlGaAs materials system and emitting in the far-infrared spectral region, i.e., below the optical phonon energy, have proved to be particularly suitable for observing the effects of in-plane magnetic confinement.[8-11] Indeed, it was demonstrated that the lifetime of the fundamental LL associated with the upper state of the radiative transition could be efficiently modulated depending on whether in or out of resonance with a LL originating from the lower state. In particular, at the condition corresponding to antiresonance between the LL's, a substantial increase of the upper state lifetime was found. These results suggested that quantization of in-plane electronic motion could be an efficient way to control and possibly improve the population inversion.[12]

In this Rapid Communication we address this issue precisely by discussing the effects of a magnetic field on the lasing properties of a copy of a recently demonstrated chirped-superlattice quantum cascade laser (QCL) emitting at 4.4 THz.[13] We show how the population inversion can be substantially modified owing to a modulation of the upper state lifetime produced by inter-LL resonances. This leads to dramatic oscillations of the threshold current density and the emitted output power with B field. In particular we observe a decrease of the threshold current density by almost 50% from 0 T to 4.3 T.

The QCL active region consists of 104-repeated periods of a GaAs/$Al_{0.15}Ga_{0.85}As$ chirped superlattice.[13] In Fig. 1 we show the band diagram of one period of the active region, obtained from a self-consistent Schroedinger-Poisson calculation, under an electric field of 3.5 kV/cm. Also shown the squared moduli of the most relevant wave functions. The energy difference between the upper and lower state of the

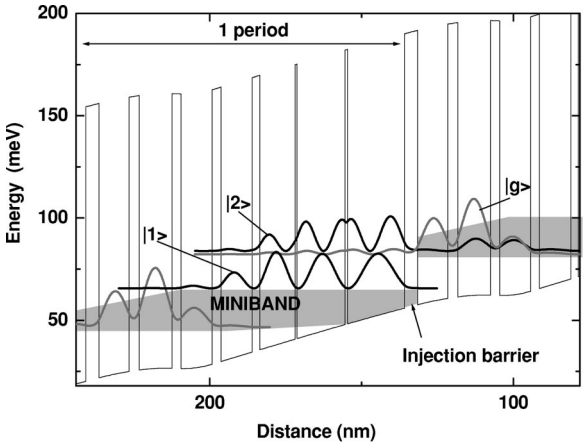

FIG. 1. Calculated band diagram, and squared moduli of the most relevant wave functions, under an electric field of 3.5 kV/cm. The two solid black lines relate to the upper and lower state of the laser transition, labeled $|2\rangle$ and $|1\rangle$ respectively. The shaded regions represent the superlattice miniband, with the ground state $|g\rangle$ depicted in gray.

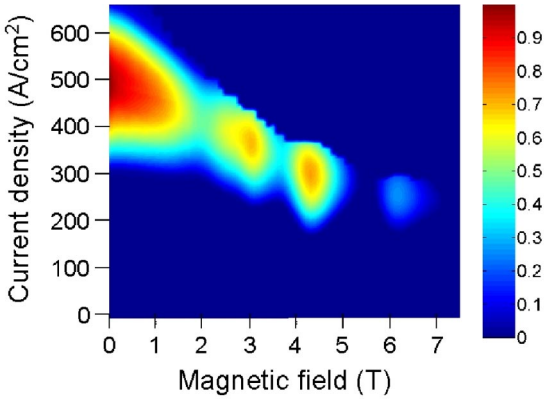

FIG. 2. (Color online) Output power in arbitrary units as a function of current density and magnetic field (T=4 K). Intensity steps beyond saturation are a consequence of curtailing the power measurements at different current densities.

laser transition, labeled $|2\rangle$ and $|1\rangle$ respectively, is equal to 18.2 meV.[14] $|1\rangle$ is the highest-lying state of the superlattice miniband, comprising seven subbands spanning an energy range of 17 meV. Electrons populating the ground state of the miniband, $|g\rangle$, are injected into state $|2\rangle$ via resonant tunneling through a 4.3 nm thick $Al_{0.15}Ga_{0.85}As$ barrier (see Ref. 13 for further details).

Lasers were processed into 60-μm wide, 2.5 mm-long ridge waveguides.[15] They were soldered to a copper holder, wire-bonded and mounted on the cold-head of a helium-flow cryostat, where a magnetic field was applied parallel to the growth axis by a split-pair superconducting coil. Light was collected from the sample and refocused on a helium-cooled composite silicon bolometer placed outside the cryostat.

In Fig. 2, we show an intensity plot of the collected power (P) as a function of current density (J) for magnetic fields from 0 to 7.5 T in steps of 0.1 T. The laser was driven in pulsed mode with a 2.5% duty cycle and a 1.5 μs pulsewidth. Measurements were performed at 4 K using standard lockin detection.

Starting from 0 T, the output power oscillates with increasing magnetic field producing four distinct local maxima. These are associated with minima in the threshold current density and vice-versa. Up to 5.3 T the magnitude of the threshold current density is found to be always lower than the 290 A/cm^2 measured at 0 T, and at 4.3 T it reaches a minimum value of 160 A/cm^2. Between 5.3 and 5.7 T and above 7.2 T, lasing action is completely quenched. Along with Refs. 8–11 we interpret these effects as a direct consequence of inter-LL resonances. These are illustrated in Figs. 3(a)–(d).

When a magnetic field is applied, the i-th subband breaks into a ladder of 0D LL's $|i, n\rangle$ with energies:

$$E_{i,n} = E_i + \hbar\omega_c \cdot \left(n + \frac{1}{2}\right), \qquad (1)$$

where $n=0, 1, 2,...$, $\omega_c = eB/m^*$ is the cyclotron frequency, and E_i is the subband energy when $B=0$ T.[16] Neglecting the term $1/2\,\hbar\omega_c$, and setting $E_{1,0}=E_1=0$ meV, in Fig. 3(a) LL energies are plotted as a function of magnetic field. $E_{2,0}$ is

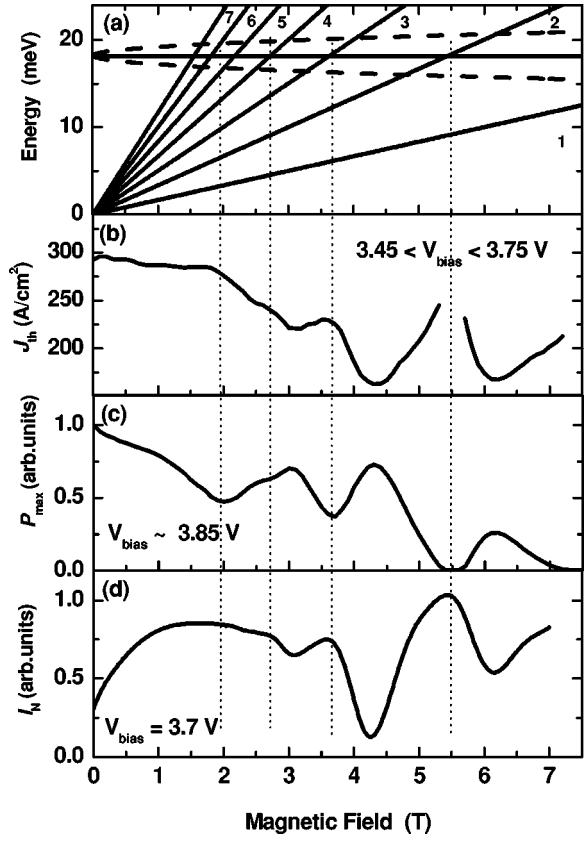

FIG. 3. (a) Energy of the most relevant LL's as a function of the magnetic field. Following Eq. (1) and neglecting the term $1/2\,\hbar\omega_c$, we set $E_{1,0}=0$ meV and $E_{2,0}=18.2$ meV (horizontal line). Lines with different slopes represent energies $E_{1,n}$ of LL's with indexes $n=1,2,...,7$. Dashed lines show the typical broadening of an individual LL.[15] (b) Threshold current density as a function of magnetic field. (c) Maximum output power as a function of magnetic field. (d) Normalized current (I_N) as a function of magnetic field at a constant bias voltage of 3.7 V. This curve was obtained from the experimental data by subtracting the decaying background current. The increase in current below 1.5 T is an artifact of background subtraction.

thus equal to 18.2 meV, whilst diagonal lines correspond to energies $E_{1,n}$ of LL's $|1, n\rangle$ with n=1,2,...,7. These have been calculated by means of Eq. (1) with $m^*=0.069\cdot m_0$, i.e., using the electronic in-plane effective mass ratio. Following Ref. 17, this is a very good approximation for the magnetic fields of interest. The two dashed lines for LL $|2, 0\rangle$ illustrate how a single LL broadens with increasing magnetic field, scaling as $\delta\sqrt{B}$, with $\delta=1$ meV/T$^{1/2}$.[18]

Figures 3(b) and (c) show the threshold current density (J_{th}) and maximum output power ($P_{\max}$) as a function of magnetic field plots, as obtained from Fig. 2. As indicated by the vertical dashed lines, peaks in J_{th} (minima in $P_{\max}$) occur at $B\cong 2.7$, 3.7, and 5.5 T, and correspond to the condition $E_{2,0}=E_{1,n}$ with $n=2$, 3, and 4 respectively. At $B=2.0$ T, we observe a broad minimum in $P_{\max}$, together with a less pronounced maximum in J_{th}. Considering the line broadening induced by the magnetic field, these features correspond to intercepts between $E_{2,0}$ and the $E_{1,5}$ and $E_{1,6}$ lines.

The excellent agreement between peak/trough positions

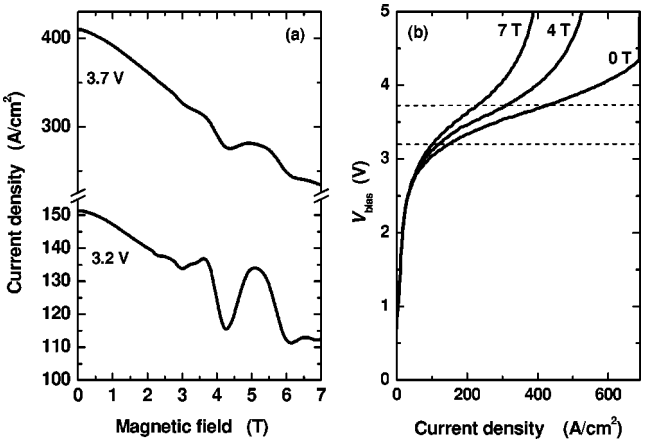

FIG. 4. (a). Current density as a function of magnetic field at constant biases of 3.2 and 3.7 V. Oscillations results from inter-LL resonances, whilst the constant decay occurs because of the reduction of nonradiative relaxation with increasing magnetic field. The relative amplitude of the oscillations is reduced at high biases owing to the decrease in the injection efficiency. (b) Voltage as a function of current density characteristics at $B=0$, 4, and 7 T. Horizontal lines indicate the bias voltages at which the two curves of panel (a) were measured.

and calculated intercept points shows that oscillations in J_{th} and $P_{\max}$ result from inter-LL resonances. In fact, when $B>0$, lasing action occurs between LL's $|2,0\rangle$ and $|1,0\rangle$. Now, whenever $E_{2,0}=E_{1,n}$, an additional path opens up for electrons in state $|2,0\rangle$ to resonantly scatter into state $|1,n\rangle$ and subsequently relax into the lower lying LL's (Note: coherent tunneling from $|2,0\rangle$ to $|1,n\rangle$ is forbidden owing to the change in Landau index). This process yields an increase of the *total* scattering rate $\tau_{2,0}^{-1}$ from state $|2,0\rangle$, i.e., a lowering of the population inversion below threshold.[19] Hence, a maximum is seen in the threshold current density, since

$$J_{th} \propto \frac{1}{\tau_{2,0}} \cdot \left(1 - \frac{\tau_{1,0}}{\tau_{2,0\rightarrow 1,0}}\right)^{-1}, \qquad (2)$$

where $\tau_{2,0\rightarrow 1,0}$ is the scattering lifetime from $|2,0\rangle$ to $|1,0\rangle$ only, whilst $\tau_{1,0}$ is the lifetime of $|1,0\rangle$.[20] The opposite effect takes place whenever $E_{2,0}$ is between $E_{1,n}$ and $E_{1,n+1}$. In this case $\tau_{2,0}$ is increased compared to its value at resonance, leading to minima in J_{th}.

Quantitative information from Fig. 3(b) could be extracted only from a complete model accounting for the correct scattering mechanism between LL's. To date, this has not been clearly identified, although recent experimental results seem to rule out carrier-carrier in favor of interface roughness and impurity scattering (see Ref. 7 and references therein).

Insight into the dependence of $\tau_{2,0}$ can be obtained by considering the variation of current density with magnetic field (J/B) at constant voltage. In fact, assuming that the majority of carriers is injected into $|2,0\rangle$, a component of the total current flow is expected to oscillate with $\tau_{2,0}$. This is displayed in Fig. 4 (a), where we show the J/B characteristics at constant biases of 3.2 and 3.7 V. The current density shows pronounced oscillations in the region 2–7 T, which are superimposed on a monotonic decrease of the current (positive magnetoresistance). As discussed at the beginning of this article, the latter effect is a consequence of the quenching of intersubband relaxation as a result of the additional in-plane quantization [see also Fig. 4 (b)].[1–3,7–9] In particular, this process produces an increase in the upper state lifetime and this is indeed the reason why the magnitude of J_{th} when $B>0$ T is always reduced with respect to the $B=0$ T case notwithstanding inter-LL resonances (the interpretation of lasing quenching between 5.3 and 5.7 T and above 7.2 T is given below).

To better identify the positions of the peaks in the J/B curves, we subtracted the decaying background from the measured J/B characteristics. The result is displayed in Fig. 3(d) for the J/B curve at 3.7 V.[21] By comparing with Fig. 3(b), we observe that minima and maxima in J and J_{th} are *perfectly coincident*, strengthening the interpretation that oscillations in the threshold current density are mainly dictated by $\tau_{2,0}$ (the current increase from 0 to 1.5 T is an artifact of background subtraction).

From Eq. (2), the threshold current density is also affected by changes in $\tau_{1,0}$. As for $\tau_{2,0}$, when $|1,0\rangle$ is resonant with a LL originating from states within the miniband, $\tau_{1,0}$ should be reduced. In this case, this process should result into minima of the threshold current density. Unfortunately, contrary to the laser transition energy, it is impossible to directly probe the energy separation between $|1,0\rangle$ and states in the miniband, therefore one has to rely on band diagram calculations. Indeed, by computing self-consistently the band diagrams at the measured bias voltages, we find resonances that are in fair agreement with the position of the observed minima in J_{th}.[22] However, we believe that the exact coincidence between minima in J and J_{th} is a strong indication that these are predominantly determined by an increase in $\tau_{2,0}$ rather than by a decrease of $\tau_{1,0}$.[23] By inspection of Eq. (2), the weak influence of $\tau_{1,0}$ on the threshold current could be explained by a low value of the ratio $\tau_{1,0}/\tau_{2,0\rightarrow 1,0}$. As a consequence, even relatively large variations in $\tau_{1,0}$ would have a small effect on J_{th}. In the absence of magnetic field, and for a structure nominally identical to the present one, the ratio $\tau_1/\tau_{2,1}$ was estimated to be ~ 0.25.[24,25] In the presence of magnetic field, this value is likely to be further reduced owing to the increase of $\tau_{2,0\rightarrow 1,0}$.

As for J_{th}, current maxima are found whenever $E_{2,0}=E_{1,n}$, showing that $\tau_{2,0}^{-1}$ is modulated by inter-LL resonances involving states $|2\rangle$ and $|1\rangle$ only. It is nevertheless worth stressing that this conclusion is not trivial since in principle one can expect $\tau_{2,0}^{-1}$ to be influenced by resonances with LL's from the other subbands forming the superlattice miniband.[13] However, from band structure calculations we find that subband $|2\rangle$ mainly overlaps with subband $|1\rangle$, and this favors scattering between LL's $|2,0\rangle$ and $|1,n\rangle$.[4,7]

From the J/V characteristics at different magnetic fields a *constant* bias voltage $V_{\rm sat}\cong 3.85$ V was derived where $P=P_{\max}$. In principle, since the energy differences between LL's change with magnetic field, there is no reason to expect the same bias voltage for the onset of power saturation.

Therefore, our finding supports the picture of electrons being resonantly injected from LL $|g, 0\rangle$ into LL $|2, 0\rangle$. In fact these two states undergo the same energy shift with magnetic field, i.e., their energy difference can be affected only by changing the bias. In particular, when $V_{bias} > V_{sat}$, $|g, 0\rangle$ and $|2, 0\rangle$ start to misalign, worsening the injection process and decreasing the emitted power. A clear signature of the decreased injection efficiency at high biases is the pronounced reduction in the relative amplitude of the current density oscillations going from 3.2 to 3.7 V [Fig. 4(a)].

Owing to positive magnetoresistance, the current at which $V \cong V_{sat}$ is progressively reduced with increasing B field. This process causes the reduction in P_{max} with respect to $B = 0$, despite the reduction in the threshold current density [Fig. 3 (c)]. Eventually, at high magnetic fields, even when $|g, 0\rangle$ and $|2, 0\rangle$ are perfectly aligned, the number of electrons injected into the upper state is not sufficient to achieve the needed degree of population inversion and lasing is suppressed, as between 5.3 and 5.7 T. This gives a full explanation of the observed experimental results.

In conclusion, we have shown how the characteristics of a 4.4 THz QCL can be substantially modified by the introduction of an additional in-plane confinement which, in the present case, was achieved by applying a magnetic field parallel to the growth axis. In particular, by simply changing the intensity of the magnetic field, one can tune the degree of population inversion. This gives rise to a reduction of the threshold current density by almost a factor of 2 from 0 to 4.3 T. Comparison with magneto-transport measurements indicate that this effect is predominantly due to an increase of the upper state lifetime, although influence from the lower state lifetime cannot be excluded. The reduction in threshold current density is counterbalanced by a progressive decrease of the vertical conductivity with magnetic field, which substantially limits the current density dynamic range before the onset of power saturation.

We gratefully acknowledge Carlo Sirtori and Cyrille Becker for helpful discussions and constant encouragement. This work was supported in part by the European Community through the IST Framework V FET project WANTED. We also acknowledge support from the EPSRC (UK), the Royal Society, Toshiba Research Europe Ltd., and Fondazione Cassa di Risparmio di Pisa (TeraLight project).

*Corresponding author. Email address: stefano.barbieri@teraview.co.uk

[1] W. M. Shu and X. L. Lei, Phys. Rev. B **50**, 17 378 (1994).
[2] H. Noguchi, H. Sakaki, T. Takamusu, and N. Miura, Phys. Rev. B **45**, 12 148 (1992).
[3] H. Hutchinson, A. W. Higgs, D. C. Herbert, and G. W. Smith, J. Appl. Phys. **75**, 320 (1994).
[4] R. Ferreira, Phys. Rev. B **43**, R11 (1991).
[5] D. Smirnov, C. Becker, O. Drachenko, V. V. Rylkov, H. Page, J. Leotin, and C. Sirtori, Phys. Rev. B **66**, 121305(R) (2002).
[6] L. Canali, M. Lazzarino, L. Sorba, and F. Beltram, Phys. Rev. Lett. **76**, 3618 (1996).
[7] K. Kempa, Y. Zhou, J. R. Engelbrecht, P. Bakshi, H. I. Ha, J. Moser, M. J. Naughton, J. Ulrich, G. Strasser, E. Gornik, and K. Unterreiner, Phys. Rev. Lett. **88**, 226803 (2002).
[8] J. Ulrich, R. Zobl, K. Unterreiner, G. Strasser, and E. Gornik, Appl. Phys. Lett. **76**, 19 (2000).
[9] S. Blaser, M. Rochat, M. Beck, and J. Faist, Phys. Rev. B **61**, 8369 (2000).
[10] B. S. Williams, H. Callebaut, Q. Hu, and J. L. Reno, Appl. Phys. Lett. **79**, 4444 (2001).
[11] S. Blaser, M. Rochat, M. Beck, D. Hofstetter, and J. Faist, Appl. Phys. Lett. **81**, 67 (2002).
[12] A. Blank and S. Feng, J. Appl. Phys. **74**, 4795 (1993).
[13] R. Köhler, A. Tredicucci, F. Beltram, H. E. Beere, E. H. Linfield, A. G. Davies, D. A. Ritchie, R. Iotti, and F. Rossi, Nature (London) **417**, 156 (2002).
[14] This value was measured at 4 K using a Fourier-transform infrared spectrometer.
[15] S. Barbieri, J. Alton, S. S. Dhillon, H. E. Beere, M. Evans, E. H. Linfield, A. G. Davies, D. A. Ritchie, R. Köhler, A. Tredicucci, and F. Beltram, IEEE J. Quantum Electron. **39**, 586 (2003).
[16] We neglected spin magnetic moment since it is irrelevant in the range of fields of interest.
[17] U. Ekenberg, Phys. Rev. B **40**, 7714 (1989).
[18] T. Ando and Y. Uemura, J. Phys. Soc. Jpn. **36**, 959 (1974).
[19] Transitions from $|1, n\rangle$ to $|1, 0\rangle$ do not contribute to the TM polarized intersubband emission.
[20] C. Gmachl, F. Capasso, D. L. Sivco, and A. Cho, Rep. Prog. Phys. **64**, 1533 (2001).
[21] From 3.2 to 3.8 V we observed a shift from 5.2 to 5.5 T in the position of the main current peak in the J/B characteristics, which is a consequence of the $\sim$1 meV stark shift of the laser transition. Points in the J_{th}/B curve of Fig. 2(b) correspond to different voltages. In particular, for points around 5 T we measured a voltage of $\sim$3.7 V. This is the reason why we used the J/B curve at 3.7 V to derive the plot of Fig. 3(d).
[22] Given the small energy separation between subbands, this type of analysis is subjected to large errors.
[23] Even in the limiting case where features in the J/B and J_{th}/B characteristics are determined by $\tau_{1,0}$, an opposite behavior is expected for the threshold current density and the total current (minima in the former should correspond to maxima in the latter).
[24] R. Köhller, R. Iotti, A. Tredicucci, and F. Rossi, Appl. Phys. Lett. **79**, 3920 (2001).
[25] R. Köhler, A. Tredicucci, F. Beltram, H. E. Beere, E. H. Linfield, A. G. Davies, D. A. Ritchie, S. S. Dhillon, and C. Sirtori, Appl. Phys. Lett. **82**, 1518 (2003).